

GeV emission from protostellar jets

Anabella Araudo^{1,2,3}, Marco Padovani⁴, Alexandre Marcowith³

¹ELI Beamlines, Institute of Physics, Czech Academy of Sciences | ²Astronomical Institute, Czech Academy of Sciences
³Laboratoire Univers et Particules de Montpellier (LUPM) Université Montpellier | ⁴INAF-Osservatorio Astrofisico di Arcetri

Introduction

Synchrotron radio emission has been detected in several protostellar jets termination region, indicating the presence of relativistic electrons (e.g. Purser et al. 2016).

- The energy density in relativistic electrons needed to explain the synchrotron flux ($> 10^{-8}$ erg cm⁻³) is significantly larger than the CR energy density in molecular clouds ($\sim 10^{-12}$ erg cm⁻³), indicating local acceleration of particles.
- Magnetic fields in the synchrotron emitter have strengths $B_s \approx 1\text{--}10$ mG. These values are larger than the expected field in the jet termination region ($B_j \approx 1\text{--}100$ μ G), indicating that an amplification mechanism is operating.

Araudo et al. (2021) study magnetic field amplification and gamma ray emission in a sample of 11 non-thermal lobes. We present here the three most prominent cases: IRAS 16547 N4, IRAS 16547 S1, and IRAS 16484 NE. We consider particle acceleration in the jet reverse shock (with velocity v_{rs}) and magnetic field amplification through Bell non-resonant hybrid instability (Bell 2004). Our scenario is sketched in Figure 1. We assume $v_{rs} = v_{jet} = 1000$ km s⁻¹, where v_{jet} is the jet velocity.

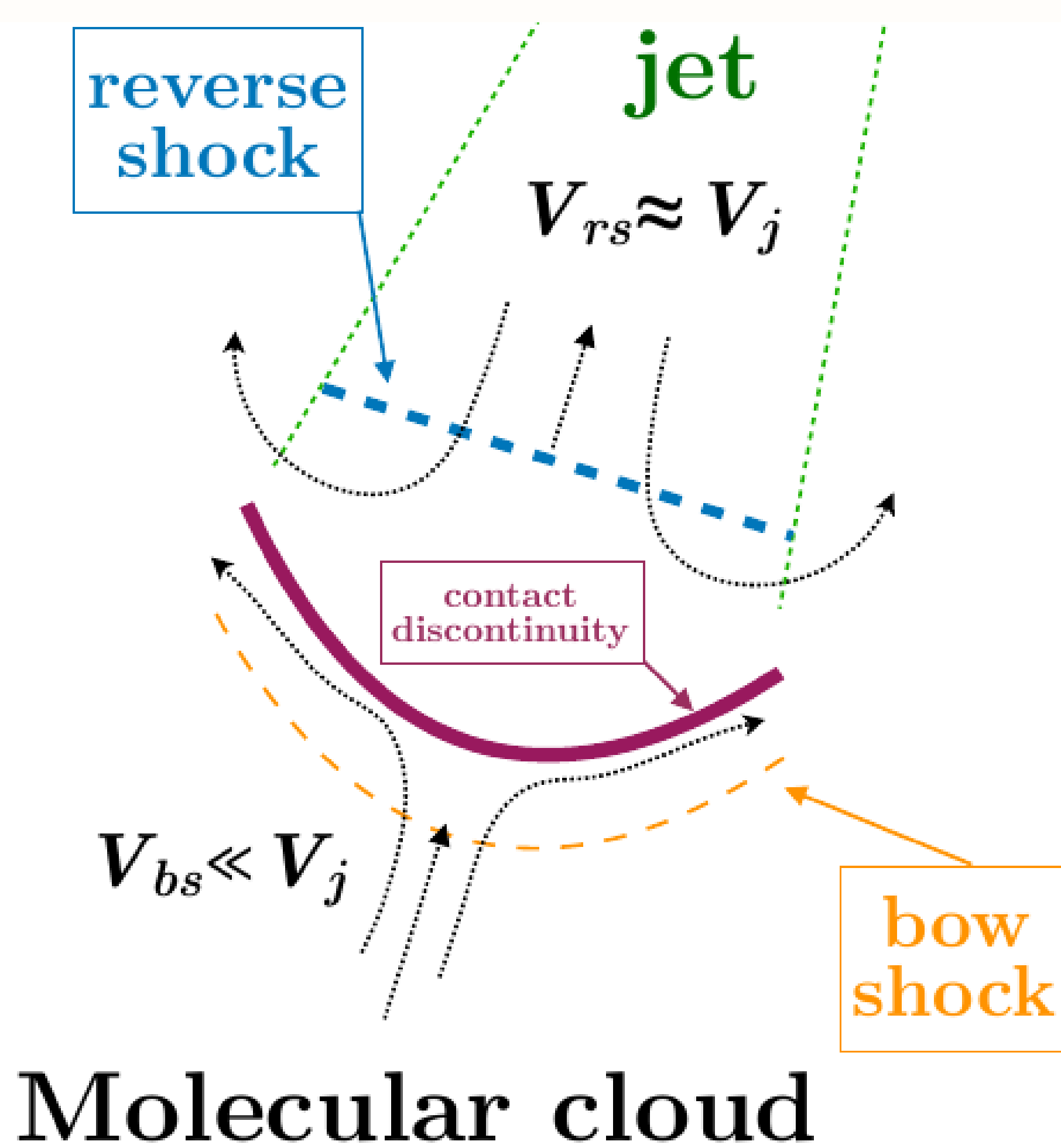


Figure 1: Sketch of the jet termination region.

Non-thermal energy content

For electrons following a distribution $N_e \propto E_e^{-s}$ the energy density is $U_{e,tot} \propto B_s^{(s-1)/2}$. The magnetic field in equipartition with relativistic electrons and protons is $B_{eq} = (1 + \alpha)^{1/2} B_{eq,e}$, where $B_{eq,e}$ is the field in equipartition with relativistic electrons only. We assumed that the energy density in relativistic protons in $U_{p,tot} = \alpha U_{e,tot}$, where α is tabulated in Table 1 together with s , B_{eq} , and the jet ion density n_i . In Fig. 2 we plot $U_{p,tot} \propto B_s^{(s-1)/2}$ (solid lines) for $B_{min} \leq B_s \leq B_{eq}$, where B_{min} is the field corresponding to the case $(1 + 1/\alpha)U_{p,tot} = U_{kin}$ and $U_{kin} = 0.5m_p n_i v_{jet}^2$ is the jet kinetic energy density. (The ionized density in the jet termination region was estimated with the mass-loss rate measured from thermal radio emission and the size of the lobe.)

Table 1: Physical parameters

Source	s	a	n_i [cm ⁻³]	B_{eq} [mG]	$B_{sat,d}$ [mG]	$E_{p,max}$ [TeV]
IRAS 16484 NE	1.78	15.06	8×10^4	14.6	1.6	0.28
IRAS 16547 N4	2.34	10.80	2×10^4	10.2	1.2	0.17
IRAS 16547 S1	1.89	63.07	8×10^3	9.93	1.1	0.43

Magnetic field amplification

The distribution of relativistic protons driving the current spans from ≈ 1 GeV to $E_{p,max} \approx 1$ TeV and therefore the (total) saturated magnetic field $B_{sat,NR}$ immediately upstream of the shock is better estimated by considering the total proton population with energy density $U_{p,tot}$. In the non-linear regime of the Bell instability, the amplified magnetic field saturates at

$$\frac{B_{sat,NR}}{\text{mG}} \approx 0.3 \left(\frac{U_{p,tot}}{10^{-6} \text{ erg cm}^{-3}} \right)^{1/2} \left(\frac{v_{rs}}{1000 \text{ km s}^{-1}} \right)^{1/2} \quad (1)$$

The isotropic upstream random magnetic field is compressed by the shock by a factor ≈ 3.3 when the shock compression ratio is 4. Therefore, the amplified field downstream of the shock is $B_{sat,d} = 3.3 B_{sat,NR}$. In Fig. 2 we plot $U_{p,tot}$ in Eq. (1) (black-dashed line) and assuming that $B_{sat,d} = B_s$. We find that

$$\frac{B_{sat,d}}{B_{eq}} \sim 0.38 \xi_{sat}(s) \left(\frac{v_{rs}}{1000 \text{ km s}^{-1}} \right)^{\frac{2}{s+5}} \quad (2)$$

and

$$\frac{U_{p,tot}}{\text{erg cm}^{-3}} = 2 \times 10^{-6} \xi_{sat}^2 \left(\frac{v_{rs}}{1000 \text{ km s}^{-1}} \right)^{\frac{-s+1}{s+5}} \left(\frac{B_{eq}}{\text{mG}} \right)^2, \quad (3)$$

where $\xi_{sat} = 10^{0.42(s-2)/(s+5)}$. Black circles in Fig. 2 indicate these values. (See also Table 1.)

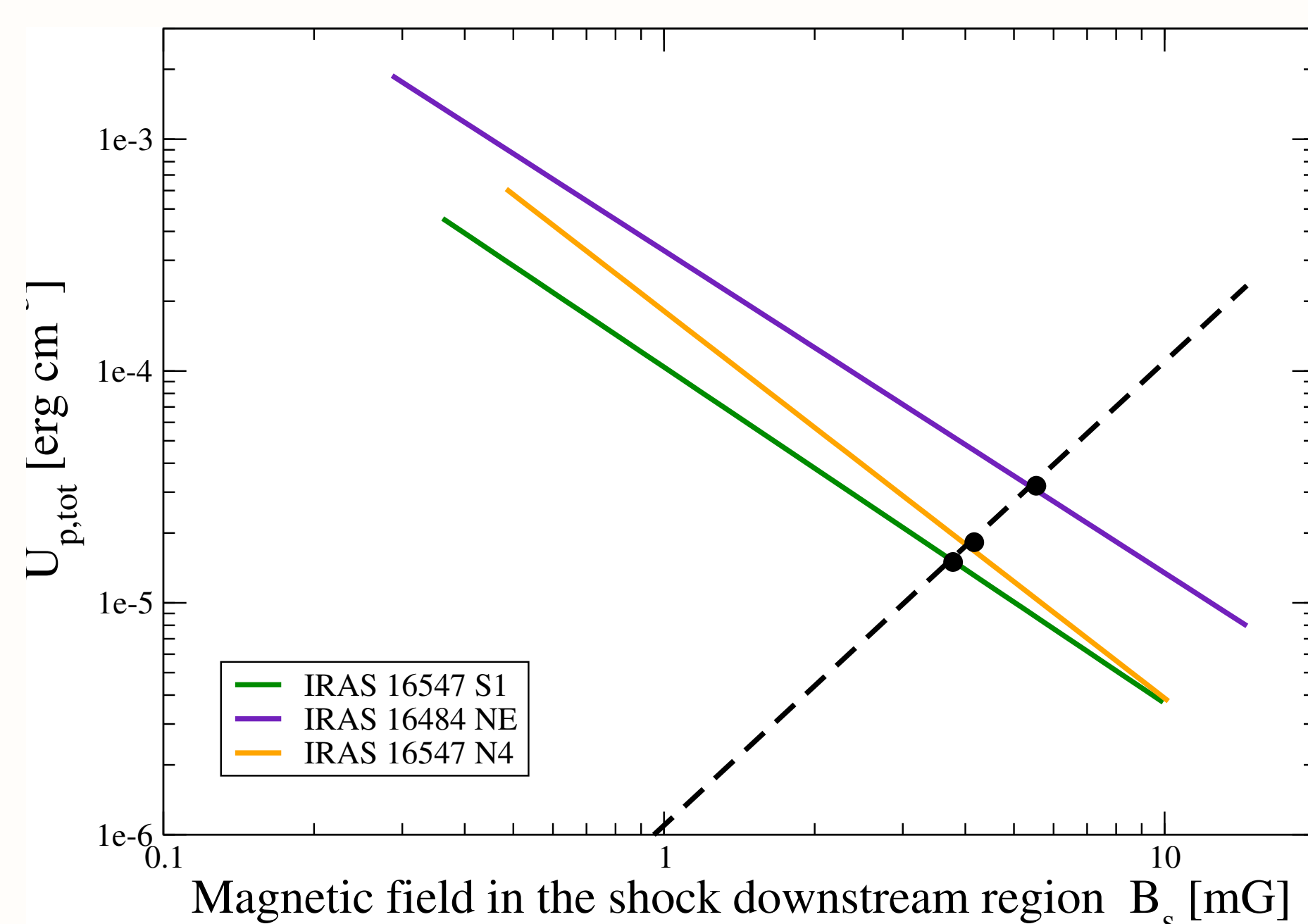


Figure 2: Determination of the magnetic field in the synchrotron emitter

Maximum energies and gamma-ray emission

The maximum energy of protons ($E_{p,max}$) is determined by the amount of protons that escape from the shock upstream region. Given that only the most energetic protons can penetrate far upstream from the shock and amplify the magnetic field in the shock precursor, the available time to accelerate these particles is $\sim 5/\Gamma_{max,NR}(E_{p,max})$, where $\Gamma_{max,NR}(E_{p,max})$ is the maximum growth rate of NR modes driven by protons with an energy $E_{p,max}$. We find $E_{p,max}$ by equating $5/\Gamma_{max,NR}(E_{p,max}) = R_j/v_{rs}$, where $R_j \sim 10^{16}$ cm is the width of the jet. Electrons behave as test particles in the magnetic turbulence created by protons. Therefore, $E_{e,max}$ is expected to be $\leq E_{p,max}$.

TeV electrons and protons emit gamma-rays by their interaction with ambient cold protons through relativistic Bremsstrahlung and proton-proton (pp) collisions. In Fig. 3 we plot the spectral energy distribution in the one-zone approximation and assuming $E_{e,max} = E_{p,max}$ (see the details in Araudo et al. 2021). The target density for pp collisions and Relativistic Bremsstrahlung was fixed in $4n_i$.

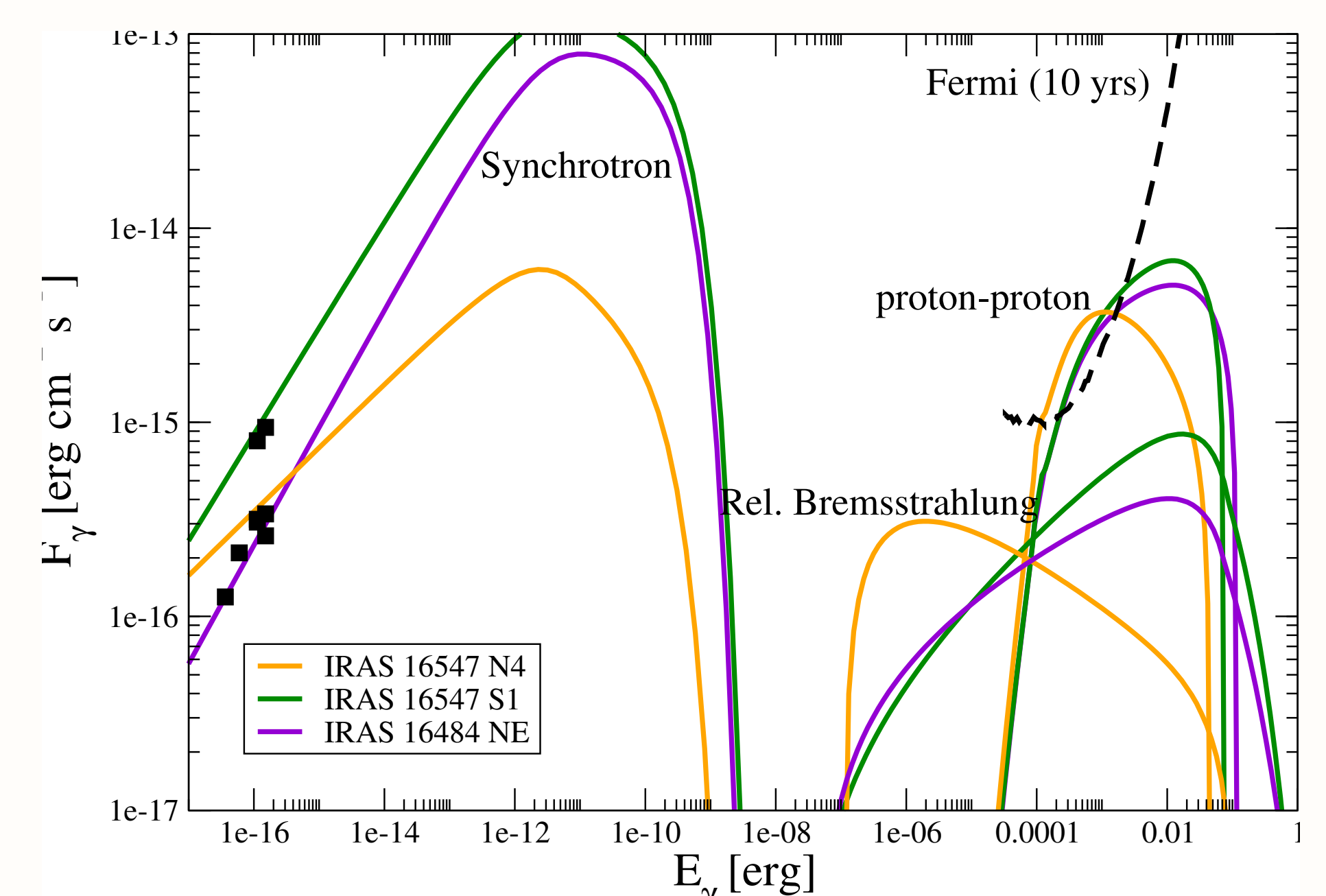


Figure 3: Spectral energy distribution for the three hot spots IRAS 16547 N4, IRAS 16547 S1, and IRAS 16484 NE. Black squares indicate radio data (Purser et al. 2016) and the black dashed line represent the *Fermi* sensitivity for 10 years of observation.

Conclusions

Under the assumption that the magnetic field in the synchrotron emitter (B_s) is amplified through the Bell's instability and fixing $v_{rs} = 1000$ km s⁻¹ we estimate $B_s \sim 0.4 B_{eq} \sim 1$ mG and the energy density in non-thermal protons $U_{p,tot} \sim 10^{-5}$ erg cm⁻³. We estimate the proton acceleration efficiency $\eta_{p,tot} = U_{p,tot}/U_{kin} \sim 0.05$. We stress that this method is different with respect to that used in supernova remnants, where the magnetic field is usually estimated by comparing the width of X-ray filament profiles with the synchrotron cooling length.

We find that having a density $n_i \sim 10^4$ cm⁻³ in the jet termination region is high enough to reach detectable levels of gamma rays with *Fermi* in IRAS 16547 N4, IRAS 16547 S1, and IRAS 16484 NE, as we show in Fig. 3. Although there is no claim of detection of these sources by *Fermi*, we expect that our result will motivate a future study on the *Fermi* data at the location of these sources. In addition, these sources will be perfect targets for a point-source mode. We also note that mixing due to Rayleigh-Taylor and thermal instabilities can significantly enhance the density of targets in the lobes. The very dense shell formed downstream of the radiative bow shock is unstable and fragmented in clumps with density $\sim 100\text{--}1000$ times the density of the ambient medium (i.e. the molecular cloud). This mixing will make other sources studied by Araudo et al. (2021) also detectable by *Fermi* in the GeV domain.

References

- [1] A.Araudo, M.Padovani, A. Marcowith (2021), MNRAS (in press)
- [2] Bell A. (2004) MNRAS 353, 550
- [3] Purser S. et al. (2006), MNRAS 460, 1039